

Exponentially fast Thinning of Nanoscale Films by Turbulent Mixing

M. Winkler,¹ G. Kofod,¹ R. Krastev,² S. Stöckle,³ and M. Abel⁴

¹University of Potsdam, Potsdam, Germany

²NMI Uni Tbingen, Reutlingen, Germany

³Max-Planck Institute for Colloids and Interfaces, Potsdam, Germany

⁴LEMETA - UMR 7563 (CNRS-INPL-UHP), 54504 VANDOEUVRE, France

(Dated: November 16, 2021)

Films are nanoscopic elements of foams, emulsions and suspensions, and form a paradigm for nanochannel transport that eventually tests the limits of hydrodynamic descriptions. Here, we study the collapse of a freestanding film to its equilibrium. The generation of nanoscale films usually is a slow linear process; using thermal forcing we find unprecedented dynamics with exponentially fast thinning. The complex interplay of thermal convection, interface and gravitational forces yields optimal turbulent mixing and transport. Domains of collapsed film are generated, elongated and convected in a beautiful display of chaotic mixing. With a timescale analysis we identify mixing as the dominant dynamical process responsible for exponential thinning.

PACS numbers: 47.61.-k, 47.57.Bc, 82.70.Rr, 47.51.+a

Thin film dynamics is governed by *gravitational, capillary* or *interfacial* forces, inducing the *disjoining pressure*. The latter combines long- and short-range molecular forces: electrostatic, Van der Waals (VdW), and steric forces [1–3] and strongly depends on the distance between the interacting surfaces. Whereas films on substrates are established in industry and research, freestanding thin liquid films (foam films) are important in nature and technology, but still provide a challenge in experiments and theory alike [4]. Consequently, the study of foam films is of central interest [2, 5], in particular their formation. The latter is primarily governed by the *thinning behavior*. We present a novel approach to thinning of *vertically oriented, freestanding, nonequilibrium, thermally forced* foam films (i.e. driven by a temperature gradient) [6]. By turbulent convection [7], we mix the fluid, i.e. we stretch and fold material lines [8]. This leads to entirely new dynamical behaviour as we will demonstrate below.

In the following we confront foam films *with* and *without* forcing. *Without perturbing forces*, two stable equilibria may occur, depending on the bulk solutions' chemistry and surface active agents (surfactants): Common Black Films with a thickness of more than 10 nm are formed when electrostatic interactions balance the dominant Van der Waals force, gravity, and capillarity [2]; Newton Black Films are stable with a thickness of less than 10 nm, due to repulsive short range steric forces [2]. We refer to both as Black Film (BF).

Since the BF is the stable phase, its progression into the thick film can be considered as a front propagation problem [9], with BF front velocity, or thinning speed, v_{BF} ; in contrast to other fronts (e.g. chemical, or biological), fluid is conserved: the front is limited by the bulk draining velocity of the film lying below. Therefore, the deposition of fluid in the thick bottom meniscus and the subsequent outflow dominate the thinning speed.

This in turn is effected by the foam film profile: it

consists of a large, flat bulk region and a meniscus, the Plateau border, which is much thicker, cf. Fig. 1, a. Whereas the drainage in the bulk region follows a slow Poiseuille flow [10], the main transport in the Plateau border [11], is well-known as marginal regeneration and shows a rich variety of patterns, cf. [12, 13]. Eventually, the whole film is thermodynamically stable as a BF. A slow drainage, steady-state profile and thermal effects have been predicted earlier, in experiments with evaporation and comparatively uncontrolled chemistry [1].

Here, a foam film is brought far into nonequilibrium by pointlike thermal forcing, cf. Fig. 1, b. The additional force counteracts gravitation and capillarity, and changes the dynamics from linear to exponential. After a transient period, a global convective flow with complex dynamic behavior is established, marked by two-dimensional turbulent mixing combined with surface instabilities. Image recording allows for a characterization of the flow field, global mixing properties, and eventually the thinning law, as the film progresses towards a global BF state. As it turns out, the observed behavior is generated by the unique combination of dynamical processes within the nanoscale film.

Experiment The experimental setup consists of a vertical rectangular aluminium frame with rounded corners, 45×20 mm, enclosed by an atmosphere-preserving cell with a glass window for video recording, cf. Fig. 1, for more details and video, see [12]. Both Common and Newton BF are optically transparent, and show a subtle difference in reflectivity which is not resolved by our setup. Thermal forcing is effected by inserting a cooled copper needle (radius 1 mm) at the film center ($T = -169^\circ\text{C}$). The needle enters the cell through a fitting hole. Ambient temperature was constant at 20°C , with a Rayleigh number $Ra \sim 10^6$, typical for turbulence. The temperature across the film (z -direction, cf. Fig. 1) is approximately constant, and the Marangoni number $Ma \simeq 0$ [12].

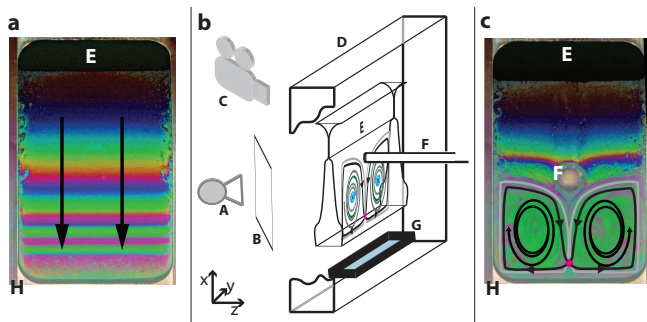


FIG. 1: The (left and right) snapshots show the reflection of a diffuse light source off the foam film surface. The color, as seen by the naked eye, repeat from top to bottom with the increasing film thickness. **a** Foam film in aluminium frame - thinning without thermal forcing. **b** Perspective view. **A**: Light source, **B**: diffusor screen, **C**: video camera, **D**: casing to prevent evaporation, with plexiglass window, **E**: BF area **F**: Cooling copper needle at -169°C , **G**: Soap reservoir, **H**: Aluminium frame. The convective pattern, established with thermal forcing is sketched, along with the BF and the thick, wedge-like region. The latter decreases in the course of time. **c** Foam film in aluminium frame - thinning with thermal forcing. The convection rolls are in the lower half of the frame, above the cold needle a stably stratified region has formed.

The solution from which the liquid film was drawn consists of the surfactant n-dodecyl- β -maltoside (β - $C_{12}G_2$), prepared with filtered deionized water and stabilized with 25 %_{vol} glycerin [14]. The entire film area is observed optically by a conventional video camera [12].

Our Vertically oriented foam film is produced initially thick (500 – 5000 nm) by pulling it with a glass rod from the reservoir, cf. [12]. Quickly, a wedge-like profile develops with BF in a small region, with a sharp horizontal boundary towards the thick film below, cf. Fig. 1, 'E'. The interference of incident and reflected light yields a striped pattern, which can be used to infer the film thickness. Each color cycle corresponds to the multiples n of the smallest negative interference condition $(2 \cdot n + 1)\lambda\eta = 4h \cos \Theta$, where the refraction index, η , is assumed to be temperature-independent; Θ is the angle of incidence [15]. The velocity is measured by color imaging velocimetry (CIV) [16] with $u \sim 0.02 \text{ m/s}$.

Results The experiments described were repeated several times in order to check reproducibility. The main sources of variation are i) initial conditions, ii) chemistry, which had been controlled by the highest accuracy known to us [14], iii) the probabilistic character of the flow, this is an intrinsic property and can only be compensated by statistical analysis.

Without thermal forcing, the initially thick film (micron scale) is drained by gravitation and capillarity, thereby evolving towards its equilibrium BF thickness. This thinning is limited by Poiseuille flow [6, 17] with the velocity $v \simeq \frac{gh^2}{2\nu}$. In the bulk, $h \sim 10^{-6} - 10^{-8} \text{ m}$,

and $v \sim 10^{-6} - 10^{-10} \text{ m/s}$. On the vertical boundaries, the so-called Plateau border with a meniscus of $h \sim 10^{-5} - 10^{-6} \text{ m}$ allows for a faster transport at $v \simeq 10^{-4} - 10^{-6} \text{ m/s}$, it is the dominant mechanism for our aspect ratio. The film in this frame reaches equilibrium, i.e. complete BF phase after approximately 5 h. A corresponding series of snapshots is given in Fig. 2, a; the dominant transport can be observed by a Kelvin-Helmholtz-like instability at the Plateau border.

We clearly observe a linear behavior with constant velocity $v_{regular} \simeq 18 \mu\text{m/s}$, in accordance with [10]. The very first quantitative thinning experiments [1] reported an exponential dynamics on the time scale of $\tau = 1000 \text{ s}$, in order to check this, we measured the thinning with open atmosphere: for our chemistry we find a slow, exponential thinning ($\tau = 4000 \text{ s}$), which we attribute to evaporation; chemistry of the surfactants plays a role, too cf. [1, 12].

With thermal forcing ((**A**) in Fig. 2 and Fig. 3), the film is cooled down rapidly in the center and a small, frozen region appears surrounding the needle. Thermal energy is exchanged at its boundaries and heavy convection starts. A weakly turbulent flow is rapidly established with 2 symmetric, dominant eddies, cf. Fig. 1, c. As a result of this convection, two different regimes are observed: faster, but still linear, and exponential thinning. We explain here the dynamics of *one* data set, presented in Fig. 2, in total we have analyzed 15 runs, all with the same reproducible dynamical behaviour [12]. Our result is a mean time constant with corresponding deviation.

In the linear regime (150 s–277 s) the velocity of the BF front is still constant, however the magnitude is increased by a factor of 3 to $v'_{BF} = 66 \mu\text{m/s}$ (cf. Fig. 3, black line). The enhancement is explained as follows: Fluid is transported by convection vertically from top to bottom, however the outflow into the reservoir is slower than the deposition rate of fluid by the convection. Necessarily, a vertical upflow at the left and right boundary is generated, causing suction of fluid from the bottom. This results in a greater, almost uniform thickness of the convection area. This increases the downward Poiseuille flow in the bulk film, such that the BF front velocity v_{BF} increases.

The second, exponential regime starts at $t \simeq 277 \text{ s}$ (**B** in Fig. 2), its dynamics is explained as follows: The BF spots arise spontaneously due to thermal and mechanical fluctuations, and are subsequently transported around by the convection. A BF spot is basically a domain of BF (5–20 nm) surrounded by much thicker film (100–1000 nm). This BF spot can only grow by transporting liquid away from the spot through the surrounding film. This transport happens again under Poiseuille flow conditions, due to the nanoscale thickness of the film.

To produce a local BF spot, mechanical and/or thermal fluctuations must exceed the energy needed to collapse. Here, we can only give an estimate, following [19]:

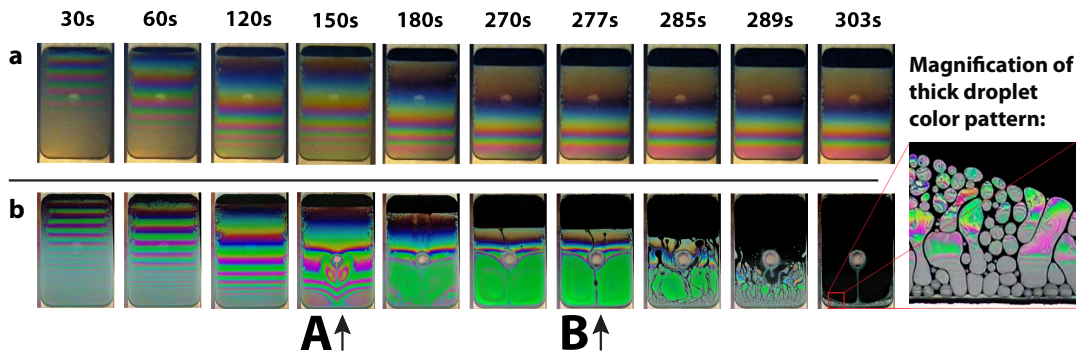


FIG. 2: **Image sequences of foam film thinning.** Thinning behaviour of a foam film **a** *without*, and **b** *with* thermal forcing. While the undisturbed thinning (top) evolves slowly, the thermally driven flow (bottom) exhibits convection, with rapid transport and mixing. **A**: start of convection, **B**: onset of exponential thinning. One clearly recognizes the black film spots which are stretched and folded, such that a rapid conversion the film evolves to the BF equilibrium phase. The magnification at the right shows the following: domains of thick film are surrounded by black film, such that the combination of forces produces an approximately spherical cap, with the lower, plane part parallel to the foam film. Consequently, the $(2n + 1)\frac{\lambda}{4}$ -condition does not hold anymore since it is based on the reflection between two parallel planes.

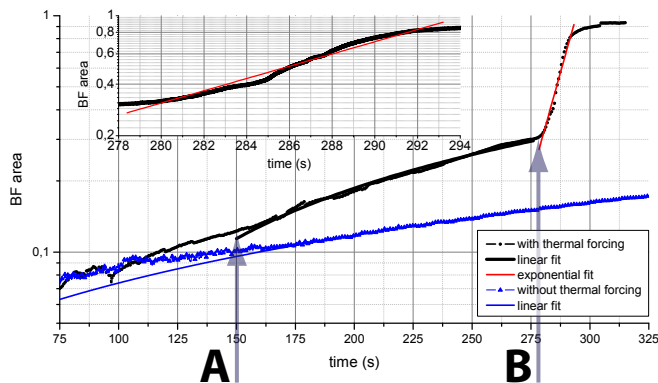


FIG. 3: **Temporal evolution of BF area: linear versus exponential thinning.** **blue triangles**: *without* thermal forcing, the thinning is perfectly linear in time. **black circles**: *with* thermal forcing, one observes three different states: for times $t < 150$ s (transition at **A**), no thermal forcing is applied and the convection has not yet started. For times $150 < t < 280$ s, the convection is established, but BF spots are not stretched into filaments, consequently thinning is linear but faster. Finally, at $t = 280$ s the transition to exponentially fast thinning can be observed, marked by **B**. BF spots and turbulent mixing are acting inside the convection zone. Solid lines are linear fits. The inset demonstrates the exponential behavior by a high-quality fit for $1 - A = \exp(-t/\tau)$, for this experiment with $\tau = 4.76$ s.

the pressure balance on the line between BF spot and surrounding thick fluid is given by $p = -\sigma \nabla^2 h - \Pi(h)$ with σ the surface tension. We estimate $\sigma \cdot \nabla^2 h \simeq 3.4$ kPa, and measured $\Pi(h)$ to be 10 kPa [12]. The pressure itself cannot be calculated analytically, however, we can estimate mechanical stresses and thermal energy per front volume as $\tau_{mech} \simeq 0.6$ Pa and $\Delta p_{thermal} \simeq 6.3$ kPa, half the pressure to overcome, $3.4 + 10 = 13.4$ kPa [12]. Fluctuations then can sometimes exceed the threshold, and the

relatively seldom occurrence of spontaneous BF formation supports our estimation.

A single BF spot is lifted up like a bubble due to gravity, and velocity gradients acting on its line interface give rise to elongation and contraction, at rate 0.3 s^{-1} and 2.52 s^{-1} , respectively. This *stretching* leads to the formation of thin BF filaments beyond a certain threshold of size and speed (cf. Fig. 2 approx. 285 s, and [12]). These filaments are then *folded* following the turbulent convection. Consequently the two basic ingredients of mixing are present, and the typical exponential separation of trajectories is reflected in the thinning law. As a result BF spots are lifted to the top to join the BF area, droplets descend due to gravity and eventually flow out into the bottom reservoir.

Now, we compare the timescales for thinning with and without thermal forcing. Essentially, the thickness varies due to i) density variation according to the local temperature; this effect is of the order $\frac{\Delta \rho}{\Delta T \cdot \alpha} \simeq 0.005$ ii) advection of h with a ratio 5/500 (final vs. initial thickness).

In the following we relate our observation to the governing dynamical equations in order to find a relation between thinning rate and convective mixing. The thinning process obeys an exponential decrease of the transient, thick phase: $\dot{A} = \gamma(A_0 - A)$, with A the area covered by thick film (Fig. 3). We find the thinning speed $v \simeq \dot{A}/L_y$ with L_y the lateral extension, and a thinning timescale, $\tau = 1/\gamma = 6.19 \pm 2.63$ s - this is 650 times faster than usual. We assumed a boundary approximately normal to gravity and space directions as indicated in Fig. 1, b.

On the other hand, the change of BF area is reflected in the change of local “control” volumes $dV = h(x, y)dA$: since the total area $A_0 = L_x \cdot L_y$ is constant, the only volume change is due to thickness evolution, such that the BF front can be obtained using $V = \int_{A_0} dx dy h(x, y)$. We are interested in the transient regime, and thus can

use the evolution equation for h given in [3]:

$$\dot{V} = \int_{A_0} dx dy \dot{h} = - \int_{A_0} dx dy h(x, y) \nabla_2 u(x, y) \quad (1)$$

with ∇_2 the two dimensional divergence and u the corresponding velocity field. Note that i) \dot{h} is the convective time derivative, i.e. the local growth and ii) the flow is highly compressible in 2D, justifying the above equation. The average thickness, denoted by brackets, evolves as $\dot{h} = -h \langle \nabla_2 u \rangle$ [18]. Identifying τ with $1/\langle \nabla_2 u \rangle$ we have related the mean convection with the thinning law. Further, we can relate this result to mixing theory [8], where the (eulerian) exponential separation of fluid points is contained in the mixing efficiency, defined as the mean stretching rate, normalized by the stretching tensor $1/2(\nabla u + (\nabla u)^T)$. Obviously, the thinning time is directly proportional to this quantity, and consequently to the mixing properties of the flow [16]. The quantitative estimate of the mixing efficiency requires more data than available, however we can test for consistency of the sign. The BF spots and filaments, respectively, expand and thus $\langle \nabla_2 u \rangle > 0$, i.e. the thickness h decreases exponentially.

We can test our approach by calculating the parameters and time scales of the involved processes: thermal forcing, gravitation, steric and electrical forces (including Van der Waals), capillarity, mechanical strain (dissipation). To estimate the important effects, we calculate Rayleigh-, Capillary-, Marangoni-, Biot-, and Prandtl numbers (Ra , Ca , Ma , B , Pr), and the dimensionless Hamaker constant \tilde{C}_H . This leads to the following values: $Ra \sim 10^6$, $Ma \sim 0$, $Ca \sim 10^{-3}$, $B \sim 10^{-4}$, $Pr \sim 17.5$, $\tilde{C}_H \sim 10^{-4}$, cf. [12], from which we deduce that the dominant force is due to temperature. The forcing produces convection, with two typical time scales: a global one, the characteristic turnover time $\tau_{conv} \sim \frac{2L}{u} \sim 5$ s and a local one, the time scale of the strain, $\tau_{strain} \sim 0.4$ s. The latter is smaller than the first, consequently the large-scale motion sets the time constant for exponential decrease of thick film area. We measure $\tau = 6.19 \pm 2.63$ s, which coincides very well with the convective scale, given the roughness of our assumptions and the complexity of the process.

Conclusion We have demonstrated the dramatic acceleration of the thinning of a foam film by thermal forcing. We use novel experimental techniques to control the properties of the thin liquid film in a precise manner, i.e. a measurement chamber that inhibits evaporation from the film surface. The analysis of the fluid flow is local and global, by tracking BF spots to measure *local* stretching, folding and *global* thinning rate.

The thermal driving leads to convection, which changes the dynamics of thinning from linear to exponential. This is not only substantially faster, but qualitatively different from the classical, thermally homogeneous, thinning process. This result can be explained: the growth of

BF area is driven by the pressure gradient at the interface with the non-equilibrium phase. Thus the interface length determines the overall thinning rate. By advection and stretching of BF spots, trails are left behind which increase multiplicatively the interface length resulting in the exponential thinning behaviour. Efficient transport and filamentation are guaranteed by the mixing properties of the flow.

We plan to widen our work to a Rayleigh-Bénard setup where the influence of interfacial forces can be studied, or, more technically, in a controlled mixing of substances in a quasi 2D setup. Further, with chemical control one can tune the film thickness and thereby observe the dependence of thermodynamical and hydrodynamical properties on the thickness, eventually testing the limits of continuum description. A comparison with quantum calculations will be a formidable task for future research.

We acknowledge initial stimulus by Nicola Abel and discussions with L. Biferale, D. Lohse, M. Sbragaglia and K.Q. Xia. This research was supported in part by the NSF under Grant No. NSF PHY05-51164 and by cost action 806 “particles in turbulence”. GK thanks the German Federal Ministry of Education and Research (BMBF) for support via grant No. 03X5511 KompAkt (WING-NanoFutur).

-
- [1] K.J. Mysels, S. Frankel, and K. Shinoda, *Soap films: studies of their thinning and a bibliography* (Pergamon Press, Oxford, 1959).
 - [2] D. Exerowa and P.M. Kruglyakov, *Foam and foam films: theory, experiment, application* (Elsevier, New York, 1998).
 - [3] A. Oron, S.H. Davis, and S.G. Bankoff, *Rev. Mod. Phys.* **69**, 931 (1997).
 - [4] G. Reiter, *Science* **282**, 888 (1998); G. M. Whitesides, *Nature* **442**, 368 (2006); F. Seychelles, Y. Amarouchene, M. Bessafi and H. Kellay, *Phys. Rev. Lett.* **100**, 144501 (2008).
 - [5] H. Kellay, X-l. Wu, and W. I. Goldburg, *Phys. Rev. Lett.* **74**, 3975 (1995).
 - [6] R. Bruinsma, *Physica A* **216**, 56 (1995); J.M. Chomaz, *J. Fluid Mech.* **442**, 387 (2001).
 - [7] G. Ahlers et al., *Rev. Mod. Phys.* **81**, 503 (2009).
 - [8] J.M. Ottino, *The kinematics of mixing: stretching, chaos, and transport*, (Cambridge Univ. Press, Massachusetts, 1989).
 - [9] W. Van Saarloos, *Phys. Rep.* **386**, 29 (2003).
 - [10] S.D. Stoyanov, V.N. Paunov, E.S. Basheva, I.B. Ivanov, A. Mehreteab, and G. Broze, *Langmuir* **13**, 1400 (1997).
 - [11] A. Saint-Jalmes, Y. Zhang, and D. Langevin, *Eur. Phys. J. E* **15**, 53 (2004); O. Pitois, N. Louvet, and F. Rouyer, *Eur. Phys. J. E* **30**, 27 (2009).
 - [12] See supplemental material. at [URL will be inserted by publisher] marginal regeneration, fluctuations; CIV; optics; dimensionless constants; video.
 - [13] V.A. Nierstrasz and G. Frens, *J. Colloid Interf. Sci.* **207**, 209 (1998).

- [14] S. Stöckle, P. Blecua, H. Möhwald, and R. Krastev, *Langmuir* **26**, 4974 (2010).
- [15] L.J. Atkins and R.C. Elliott, *Am. J. Phys.* **78**, 1248 (2010).
- [16] M. Winkler and M. Abel, *Physica Scripta* (2012) (to be published 01/13).
- [17] Y. Couder, J.M. Chomaz, and M. Rabaud, *Physica D* **37**,384 (1989).
- [18] Th. Erneux and S. H. Davis, *Phys. Fluids A* **5**,1117 (1993).
- [19] H. Diamant and O. Agam, *Phys. Rev. Lett.* **104**, 047801 (2010).